



***Sinapis alba* as an anti-rusting agent for corrosion of stainless steel in Hydrochloric acid medium**

Shwetha N¹, Padmalatha Rao^{1*}

¹Department of chemistry, Manipal Institute of Technology, Manipal, Udupi, Karnataka

Abstract: Protection against corrosion using *Sinapis alba* was studied for the corrosion control of stainless steel in 0.5M HCl. The electrochemical techniques such as potentiodynamic polarization (PDP) measurements and electrochemical impedance spectroscopy (EIS) method were used for the stainless steel protection studies. Surface morphology studies were done for the specimen immersed in the inhibitor solution and the aggressive medium. Mechanism for the corrosion inhibition was proposed. Results showed that *Sinapis alba* acted as mixed type of inhibitor, with maximum inhibition efficiency of 88% for the concentration of 0.1gL⁻¹ at 323K. It got chemically adsorbed on stainless steel by obeying Langmuir adsorption isotherm. *Sinapis alba* emerged as an effective eco-friendly corrosion inhibitor for the corrosion control of stainless steel in HCl acid medium.

Keywords: Stainless steel, Green inhibitor, *Sinapis alba*, Electrochemical measurements, SEM, EDX

1 Introduction

Stainless steel is an alloy of iron, carbon and chromium. It has wide range applications in various fields such as oil and gas industries, building and constructions. These immense applications are due to the formation of chromium oxide film on the metal surface [1-3]. But when the metals come in contact with mineral acids like hydrochloric acid and Sulfuric acid etc., especially during pickling process and there will be material loss [4].

In order to prevent the material loss, the corrosive environment can be altered by adding the corrosion inhibitors. Most commonly organic compounds containing heteroatoms like O, N, S and P are used as protective agents, but preparation of organic compounds involves toxic substances which lead to environmental hazardous [5-7]. In order to overcome this, now-a-days research is geared towards the use of green inhibitors. Green inhibitors are biodegradable, environmentally benign, inexpensive and non-toxic [8-9].

Sinapis alba is commercially called as white mustard. White mustard seeds are hard round seeds, usually around 1.0 to 1.5 mm in diameter, with pale yellow colour [10]. The major active constituent present in *Sinapis alba* is reported to be Benzyl isothiocyanate. In addition to this, *Sinapis alba* also contain large number of heterocyclic compounds like alkaloids, flavonoids etc., As a part of our research work with green corrosive inhibitors [11] we report herein the use of *Sinapis alba* as an eco-friendly corrosion inhibitor for the corrosion control of stainless steel in HCl acid medium.

2 Experimental

2.1 Material

Stainless steel material composition is given in the table 1. From this material we performed the experiment.

Table1: Composition of the stainless steel specimen.

Element	C	Si	Mn	Cr	Ni	Fe
Composition(%)	0.0450	0.332	1.97	18.33	8.43	Balance

2.2 Preparation of test coupon

Test coupon of stainless steel having 1cm² diameter with 5cm height of cylindrical rod was prepared by moulding with cold setting acrylic resin. Polishing was done with different graded emery papers and finally with disc polisher using levigated alumina to obtain mirror like surface. Then it was cleaned by double distilled water followed by acetone and dried for further use.

2.3 Preparation of medium

Acid stock solution was prepared by using 37% HCl and double distilled water. It was standardized by using previously standardized sodium hydroxide solution by volumetric titration method. The standardized stock solution was diluted appropriately to get 0.5M HCl solution.

2.4.1 Preparation of inhibitor solution

White mustard seeds were collected from the commercial store. The seeds were washed with double distilled water and dried up to 1 week without exposing light directly. Then it was finely powdered using domestic mixer grinder.

Sinapis alba seed extract (SASE) in aqueous medium was prepared by taking 25g of powdered white mustard seeds. It was refluxed in 500mL distilled water up to 5 h and kept for overnight to settle down and filtered, filtrate was collected. It was then evaporated to complete dryness at 40 °C, in order obtain brown colour solid residue. The solid residue obtained was weighed and preserved in a desiccator for further use. It was then used for corrosion inhibition studies with concentration ranging from 0.005 – 0.01 gL⁻¹.

2.5 Electrochemical Measurements

The electrochemical measurement of stainless steel in 0.5M HCl was performed by using electrochemical work station (CH600D-series, U.S. Model with CH instrument beta software). The electrochemical cell used was a conventional three electrode compartment Pyrex glass cell with platinum as counter electrode and a saturated calomel electrode (SCE) as reference electrode. Stainless steel was used as a working electrode.

2.5.1 Potentiodynamic polarisation (PDP) measurements

Potentiodynamic polarisation studies were carried out for the stainless steel in 0.5M HCl acid at different temperatures in presence and absence of inhibitor. Steady state open circuit potential was obtained at the end of 300 seconds with respect to SCE. The potentiodynamic plots were obtained by polarising the stainless steel from -250mV cathodically to +250mV anodically with respect to OCP with a scan rate of 1mVsec⁻¹. With this corresponding corrosion current density (i_{corr}), corrosion potential (E_{corr}) and Tafel slope value were obtained.

2.5.2 Electrochemical impedance spectroscopy (EIS) studies

Electrochemical impedance spectroscopy studies for stainless steel was carried out in the frequency ranging from 10000 to 0.01Hz by applying a small amplitude ac signal of 10mV at the OCP. The procedure was repeated 3-4 times and best of the three agreeing values were repeated.

2.6 Surface studies: SEM and EDX analysis

Surface morphology studies of stainless steel were carried out by immersing the specimen in 0.5M HCl in the presence and absence of SASE for 2h using analytical scanning electron microscope (JEOL JSM-6380L) and elemental mapping was done by Energy Dispersive X-ray analysis.

3 Results and discussions

3.1 Fourier transforms infrared (FTIR) spectroscopy of SASE

Figure 1 is the FTIR spectrum of solid residue of SASE. In which -N=C=S appears in the frequency range of 2360cm^{-1} . The fingerprint region at 2929cm^{-1} is for aromatic ring. The -C=C- stretching frequency appears at 1668cm^{-1} and 1541cm^{-1} respectively. The phenolic -OH stretching appears at 3618cm^{-1} . The FTIR spectrum confirms the presence of electron rich heteroatoms.

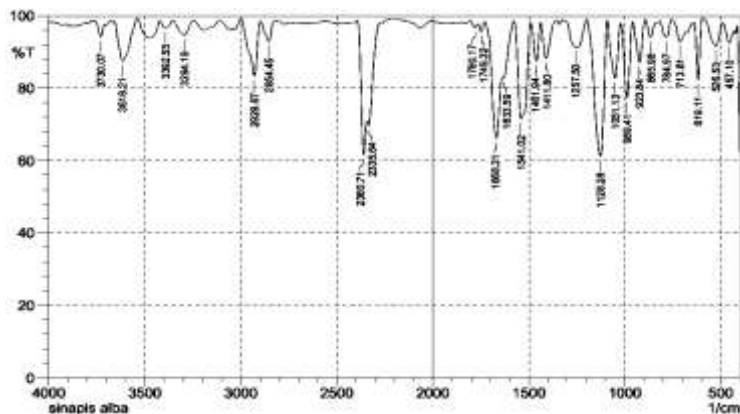


Fig1: IR spectrum of solid residue of SASE

3.2 Electrochemical measurements

3.2.1 Potentiodynamic polarisation (PDP) measurements

Figure 2 shows the Potentiodynamic polarization plots for stainless steel 0.5M HCl with various concentrations of SASE along with blank at Similar plots were obtained at different temperatures. Figure 2 shows that as the SASE inhibitor concentration increased there was a positive shift in the corrosion potential with respect to blank at $30\text{ }^{\circ}\text{C}$. This indicates that, introduction of SASE inhibitor controls the corrosion of stainless steel in acid medium. A change in the shape of anodic slope is because of passivation observed in between -0.3V to -0.1V . The cathodic polarization curves have linear behaviour and values of cathodic slope ($-\beta_c$) are not varying significantly with increase in inhibitor concentration. This indicates that the hydrogen evolution is activation-controlled and the presence of inhibitor did not alter the inhibition mechanism [12-13]. According to the literature, if displacement in corrosion potential is more than $\pm 85\text{ mV}$ with respect to corrosion potential of the uninhibited solution the inhibitor can be considered as a cathodic or anodic type of inhibitor. However, the maximum displacement in this study is not more than 85 mV , which indicates that inhibitor is act as a mixed type inhibitor [14].

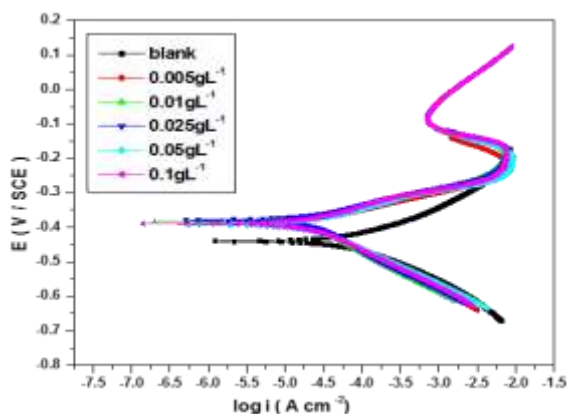


Fig 2: Potentiodynamic polarization plots for corrosion of stainless steel in 0.5M HCl containing different concentrations of SASE at $30\text{ }^{\circ}\text{C}$.

The potentiodynamic parameters for stainless steel in acid medium in the presence and absence of SASE are obtained from this study. Corrosion rate and % efficiency of the SASE was calculated using equation 1 and 2 respectively.

$$\text{CR (mmy}^{-1}\text{)} = \frac{3270 \times M \times i_{\text{corr}}}{\rho \times z} \quad (1)$$

where 3270 is a constant that defines the unit of corrosion rate, i_{corr} is the corrosion current density in Acm^{-2} , ρ is the density of the corroding material (gcm^{-3}), M is the atomic mass of the metal and Z is the number of electrons transferred per atom.

$$\text{I.E(\%)} = \frac{i_{\text{corr}} - i_{\text{corr(inh)}}}{i_{\text{corr}}} \times 100 \quad (2)$$

where i_{corr} and $i_{\text{corr(inh)}}$ are the corrosion current densities in the absence and in the presence of inhibitor, respectively. Table 2 shows potentiodynamic polarization values for stainless steel in presence and absence of SASE at different temperatures.

Table 2: Results of potentiodynamic polarization studies for corrosion of stainless steel in 0.5M HCl containing various concentrations of SASE at different temperatures

Temp (K)	[SASE] gL^{-1}	E_{corr} (mV vsSCE)	$i_{\text{corr}} \times 10^{-5}$ (A cm^{-2})	β_a (mV dec^{-1})	$-\beta_c$ (mV dec^{-1})	CR (mmy^{-1})	I.E (%)
303	Blank	-440	7.385	1023	1031	16.61	---
	0.005	-390	2.381	1938	827	5.35	67.88
	0.01	-383	2.173	1987	775	4.88	70.57
	0.025	-379	1.937	2238	781	4.35	73.77
	0.05	-393	1.784	2277	987	4.01	75.84
	0.1	-389	1.662	2393	902	3.73	77.49
308	Blank	-441	10.51	1073	1053	23.63	---
	0.005	-365	2.827	1842	783	6.35	73.10
	0.01	-408	2.580	2029	979	5.80	75.45
	0.025	-411	2.402	2230	986	5.40	77.14
	0.05	-380	2.039	2664	903	4.58	80.59
	0.1	-392	1.905	2849	1029	4.28	81.87
313	Blank	-444	14.40	1104	1080	32.39	---
	0.005	-402	3.463	2114	1038	7.78	75.95
	0.01	-373	2.793	2129	806	6.01	80.60
	0.025	-378	2.315	2428	885	4.40	83.92
	0.05	-388	2.064	2734	985	4.28	85.66
	0.1	-392	1.970	2912	1054	4.07	86.31
318	Blank	-442	15.49	1157	1047	34.83	---
	0.005	-406	3.575	1747	1040	8.04	76.92
	0.01	-396	2.676	2511	1018	6.28	82.72
	0.025	-391	1.959	2608	1072	5.20	87.35
	0.05	-392	1.905	2849	1029	4.64	87.70
	0.1	-393	1.784	2277	9879	4.01	88.48

As the inhibitor concentration increased the corrosion current density decreased. It is evident that percentage of efficiency of the inhibitor increased with increase in the concentration of SASE and also with increasing the temperature because of adsorption of inhibitor on the metal surface. The maximum inhibition efficiency 88% was observed at 45 °C for higher concentration of inhibitor of 0.1g L⁻¹. This indicates SASE gets adsorbed over the metal surface at very high temperature and protects the stainless steel from undergoing the corrosion.

3.2.2 Electrochemical impedance spectroscopy (EIS) studies

Figure 3 shows the Nyquist plot of stainless steel in 0.5M HCl with different concentrations of SASE and same plots are obtained for all temperature. The Semicircle in this plot because of charge transfer controlled process [15] and the diameter of semicircle increases with increase in inhibitor concentration indicates that inhibitor protects the metal by corrosion. The Nyquist plots with a depressed capacitive loop at high-frequency range (HF), this is because of the surface roughness, inhomogeneity of the solid surface and also the adsorption of the inhibitor on the metal surface [16]. The large capacitive loop at high frequency region indicates that charge transfer process occur during corrosion and double layer behaviour. The high frequency capacitive loop could be assigned to the charge transfer of the corrosion process and to the formation of oxide layer [17].

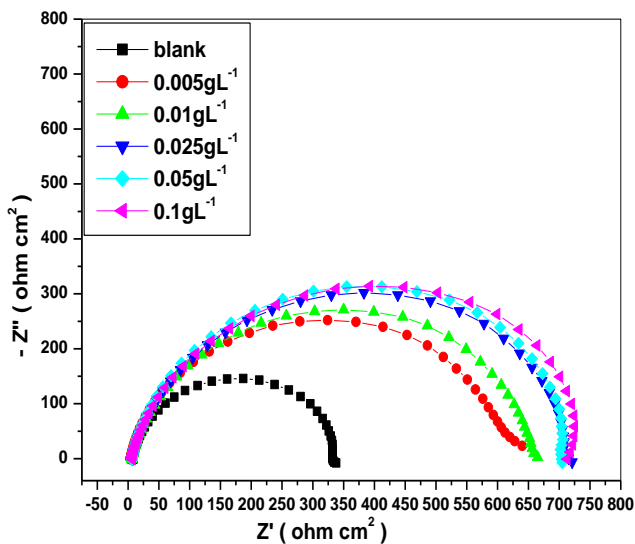


Fig 3: Nyquist plot for corrosion of stainless steel in 0.5M HCl containing different concentrations of SASE at 30 °C.

Impedance data were simulated to get appropriate equivalent circuit using 3.21 version of Zimpwin software. It is represented in Figures 4(a) and 4(b) respectively.

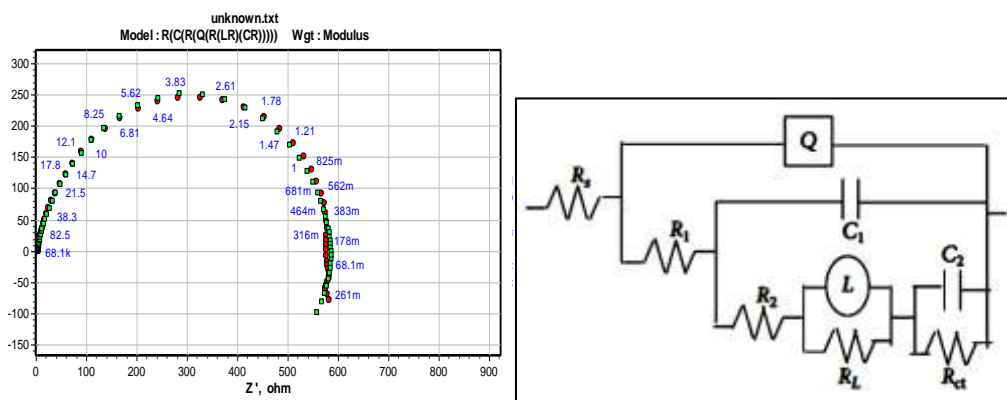


Fig4 (a): Simulated Impedance data for stainless steel corrosion in 0.5M HCl at 35°C (b) Equivalent circuit of nine elements

The equivalent circuit consists of solution resistance (R_s), charge transfer resistance (R_{ct}), Inductive resistance (R_L) and inductive element (L). It also consists of CPE (constant phase element, Q), which is parallel to the series of capacitance C_1 and C_2 and resistor R_1 , R_2 , R_L and R_{ct} and R_L is parallel to L inductor.

Double layer capacitance (C_{dl}) and polarization resistance (R_p) can be obtained by using the equations (3) and (4) respectively,

$$C_{dl} = C_1 + C_2 \quad (3)$$

$$R_p = R_1 + R_2 + R_L + R_{ct} \quad (4)$$

R_p is inversely proportional to the corrosion current and it can be used to calculate the percentage inhibition efficiency using the relation (5).

$$IE (\%) = \frac{R_{p,corr(inh)} - R_{p,corr}}{R_{p,corr(inh)}} \times 100 \quad (5)$$

where $R_{p,corr(inh)}$ and $R_{p,corr}$ are the polarization resistances in the presence and absence of inhibitor.

Table 3 shows the results obtained from electrochemical impedance spectroscopy technique. Double layer capacity was calculated using equation (6).

$$C_{dl} = Q_{dl} \times (2\pi f_{max})^{(a-1)} \quad (6)$$

Table 3: Impedance values obtained for corrosion of stainless steel in 0.5 M HCl containing various concentrations of SASE at different temperatures.

Temp (K)	[SASE] $g L^{-1}$	C_{dl} $\times 10^{-5}$ ($F cm^{-2}$)	R_p (Ωcm^2)	IE (%)
303	Blank	11.72	287	---
	0.005	10.51	660	56.5
	0.01	9.24	724	60.35
	0.025	8.55	743	61.37
	0.05	8.43	747	61.57
	0.1	6.93	794	63.85
308	Blank	16.90	195	---
	0.005	14.80	586	66.72
	0.01	11.16	560	65.17
	0.025	10.64	563	65.36
	0.05	5.95	589	66.89
	0.1	5.26	598	67.39
313	Blank	18.12	138	---
	0.005	11.70	398	75.32
	0.01	8.29	530	73.93
	0.025	7.67	556	75.17
	0.05	6.82	566	75.61
	0.1	5.42	567	75.66
318	Blank	22.61	127	---
	0.005	12.34	436	70.89
	0.01	9.95	460	72.39
	0.025	8.38	589	78.43
	0.05	6.93	604	78.97
	0.1	6.08	747	82.99

As observed in Table 3 R_p values are increased with the concentration of SASE but C_{dl} value decreased because of increase in the thickness of electrical double layer in between metal and solution interface [18]. The results of potentiodynamic polarization method showed good agreement with results of electrochemical impedance spectroscopy methods.

3.3 Effect of temperature

To understand the adsorption behaviour of SASE on stainless steel the effect of temperature was studied and the activation parameters such as energy of activation (E_a), the enthalpy (ΔH_a) and entropy of activation (ΔS_a) values was obtained from this study. The energy of activation (E_a) can be calculated from Arrhenius law equation given in the equation 7.

$$\ln(CR) = B - \frac{E_a}{RT} \tag{7}$$

Where B is Arrhenius constant which depends upon the metal type and R is equal to $8.314 \text{ JK}^{-1}\text{mol}^{-1}$, T is the absolute temperature.

Figure 5 was for Arrhenius plot of stainless steel plotted against $\ln(CR)$ versus $1/T$. Which gave the straight lines with a slope from which calculate the value of energy of activation (E_a).

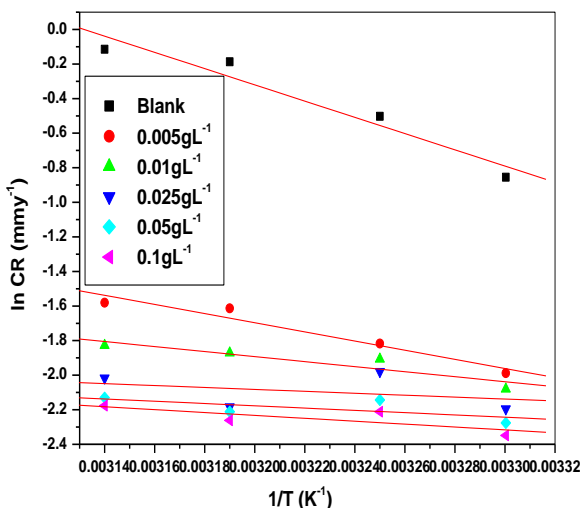


Fig 5: Arrhenius plots for the corrosion of stainless steel in 0.5M HCl at different concentrations of SASE.

The transition state equation 8 was used to calculate the enthalpy (ΔH_a) and entropy of activation (ΔS_a) for the dissolution of metal.

$$CR = \frac{RT}{Nh} \exp\left(\frac{\Delta S_a}{RT}\right) \exp\left(-\frac{\Delta H_a}{RT}\right) \tag{8}$$

where h is planks constant ($6.626 \times 10^{-34} \text{ Js}$), N is Avogadro’s number ($6.023 \times 10^{23} \text{ mol}^{-1}$).

From the plot of $\ln(CR/T)$ versus $1/T$ also gave a straight line from this straight line slope gave the value of enthalpy of activation and the intercept gave the value of entropy of activation. Figure 6 is the plot of $\ln(CR/T)$ versus $1/T$ for stainless steel in various concentration of SASE in 0.5M HCl.

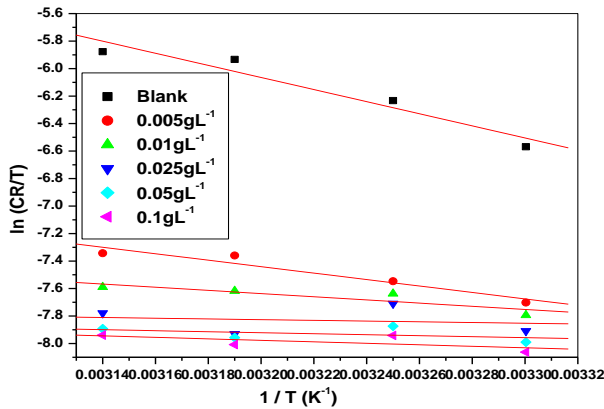


Fig 6: Plots of ln(CR/T) vs 1/T for the corrosion stainless steel in 0.5M HCl containing different concentration of SASE

Table 4: Activation parameter for the corrosion of stainless steel in 0.5M HCl containing different concentrations of SASE

[SASE] g L ⁻¹	E _a (kJ mol ⁻¹)	ΔH _a (kJ mol ⁻¹)	ΔS _a (J mol ⁻¹ K ⁻¹)
Blank	39.061	36.589	- 189.51
0.005	21.991	19.519	- 197.46
0.01	12.084	9.612	- 201.47
0.025	4.634	2.162	- 204.53
0.05	5.486	3.014	- 204.29
0.1	6.969	4.497	- 203.78

Data for the Activation parameters for corrosion of stainless steel in 0.5M HCl containing different concentrations of SASE are given in Table 4. Energy of activation (E_a) values of the stainless steel in presence of SASE is lesser as compared with absence of inhibitor. This decrease in the E_a value of the inhibited solution is indicates that chemical adsorption of the SASE inhibitor on the surface of the stainless steeland attains equilibrium at higher temperature [19, 20]. The inhibitor molecule gets chemically adsorbed on the metal surface and decreases the electrochemical corrosion process [21, 22, 23]. The positive sign of ΔH_a indicates that the endothermic process of stainless steel metal dissolution process [24]. The entropy of activation (ΔS_a) data are negative which indicates that, in rate determining step the activated complex is association not dissociation i.e. decrease in the disorderness on going from reactants towards the activated complex [25,26].

3.4 Adsorption isotherm

For understanding the mechanism of adsorption of inhibitor on metal surface and inhibition of stainless steel in acid medium we study the adsorption isotherm. The degree of surface coverage value obtained from the potentiodynamic polarisation studies were applied for various types of various adsorption isotherms such as Langmuir, Freundlich, Temkin and Frumkin and the data was best fitted with Langmuir adsorption isotherm which can be related by the relationship (9)

$$\frac{C}{\theta} = \frac{1}{K} + C \tag{9}$$

Where, K is adsorption/desorption equilibrium constant (Lmol⁻¹), C is the concentration of inhibitor molecule in the electrolyte, then θ is given by the equation (10)

$$\theta = \frac{I.E(\%)}{100} \tag{10}$$

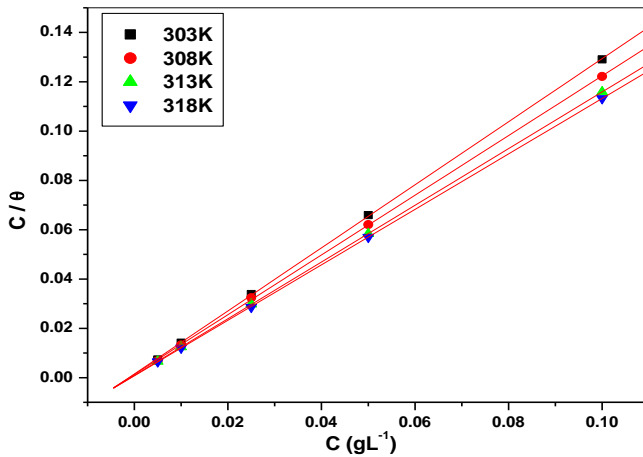


Fig 7: Langmuir adsorption isotherm for the adsorption of SASE on stainless steel in 0.5M HCl at different temperatures.

Figure 7 indicates Langmuir adsorption isotherm plot for stainless steel. The plot of $\frac{C}{\theta}$ versus C gave straight line from the intercept $\frac{1}{K}$ values were obtained. The isotherm slopes showed deviation from the value of unity as would be expected for the ideal Langmuir adsorption isotherm equation. This deviation may be because of the interaction among the adsorbed inhibitor on the metal surface. Standard free energy of adsorption (ΔG_{ads}^0) can be calculated by using the values of K, which is related by the equation (11).

$$K = \frac{1}{55.55} \exp\left(\frac{-\Delta G_{ads}^0}{RT}\right) \quad (11)$$

Where R is universal gas constant, T is the absolute temperature; the value 55.55 in the above equation is the concentration of water in the solution in mol⁻¹.

The values of Standard enthalpy of adsorption (ΔH_{ads}^0) and Standard entropy of adsorption (ΔS_{ads}^0) were obtained by plotting ΔG_{ads}^0 verses T in Figure 8. The figure 8 shows linear plot; from the slope of straight line ΔS_{ads}^0 value and from the intercept of the straight line ΔH_{ads}^0 values were calculated by using Gibbs Helmholtz equation (12).

$$\Delta G_{ads}^0 = \Delta H_{ads}^0 - T\Delta S_{ads}^0 \quad (12)$$

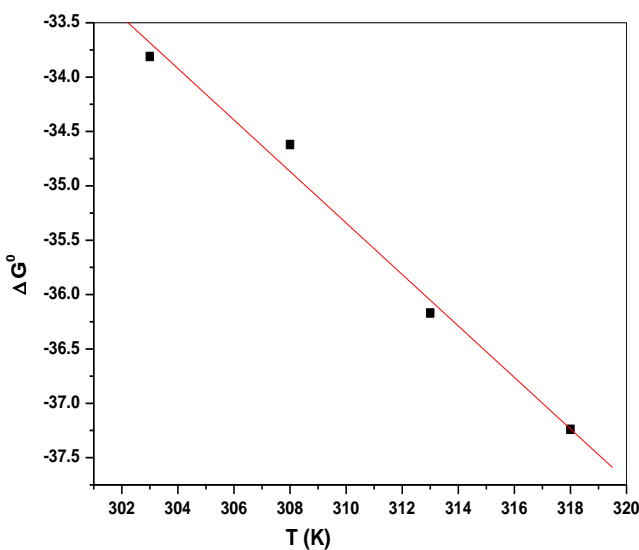


Fig 8: Plot of ΔG_{ads}^0 vs. T

When the ΔG_{ads}^0 value up to -20 kJ mol^{-1} then we considered that there is an electrostatic interaction between the negatively charged metal surface and protonated inhibitor molecule i.e. Physisorption. The value is more negative than -40 kJ mol^{-1} then considered that sharing or transfer electrons from the inhibitor molecule to the surface of the metal through coordinate bond formation i.e. chemisorption [26].

Table 5: Thermodynamic parameters of stainless steel in 0.5M HCl

Temp (K)	ΔG_{ads}^0 (kJ mol^{-1})	ΔH_{ads}^0 (kJ mol^{-1})	ΔS_{ads}^0 ($\text{kJ mol}^{-1}\text{K}^{-1}$)
303	-33.81	38.06	0.236
308	-34.62		
313	-36.17		
318	-37.24		

Thermodynamic parameters for stainless steel in 0.5M HCl are given in the table 5. The table shows that the negative value of ΔG_{ads}^0 imply inhibitor adsorption is spontaneous. The ΔG_{ads}^0 value is less than -40 kJ mol^{-1} and increased with increasing the temperature which implies that the adsorption of inhibitor increases with increasing temperatures and also the inhibitor molecules are chemically adsorbed on the surface of the stainless steel [27]. When the ΔH_{ads}^0 values less than -40 kJ mol^{-1} indicates physical adsorption of inhibitor on the metal surface and if it is in between -40 kJ mol^{-1} and -100 kJ mol^{-1} , then it is considered as chemical adsorption of inhibitor. The table shows the ΔH_{ads}^0 value is positive which clearly indicates that chemical adsorption of SAES on the surface of metal.

3.5 Mechanism of corrosion

Based on the adsorption phenomenon the corrosion inhibition of metals in acidic solution can be described. In this present study of work the adsorption of SASE on the stainless steel can be attributed to either sharing of electrons between the hetero atoms and iron or π electron interaction between the aromatic ring of the SASE and the metal surface [28].

SASE is rich in hetero atoms which have active constituent of SASE is benzyl isothiocyanate shown in Figure 9.

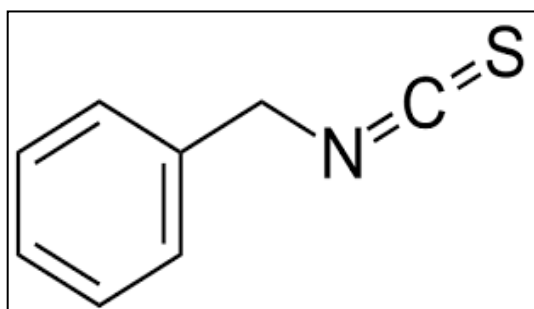
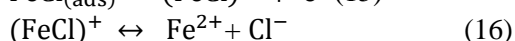
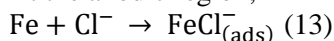


Fig 9: Structure of Benzyl isothiocyanate

The mechanism of inhibition can be predicted from the knowledge of the interaction between the inhibitor molecules and the surface of the metal. In acid solution the mechanism of dissolution of stainless steel takes place as follows.

At the anodic region;



The major cathodic reaction is evolution of hydrogen gas according to the following steps:

Table 6: EDX data obtained for stainless steel surface analysis before and after corrosion inhibition with SASE

Elements	% Composition								
	C	Si	Cl	Cr	Mn	Fe	O	Ni	Cu
Freshly polished SS	2.62	0.41	---	18.03	1.89	68.94	---	8.11	0.57
SS in 0.5M HCl	---	0.30	4.60	14.45	1.63	54.45	12.66	6.64	0.55
SS in 0.5M HCl+0.1gL ⁻¹ SASE	14.1	0.56	2.77	15.65	1.74	59.63	7.34	7.19	---

When the specimen was immersed in the corrosive, there was a peak corresponding to chlorine. (4.60%) This indicates the interaction the medium with the material and hence the corrosion of stainless steel. Corrosion of the material is evident due to decrease in the concentration of the Cr (14.45%) and Ni (6.64%). After the addition of the inhibitor, composition of chlorine is decreased (2.77%). Increase in the composition of carbon content (14.1%) confirms the adsorption of the inhibitor on the metal surface.

4 Conclusion

- Inhibition efficiency of SASE increased with increase in the concentration of inhibitor and with increase in temperature.
- SASE acted as a mixed type of inhibitor for stainless steel in 0.5M HCl medium.
- SASE got chemically adsorbed on the metal surface and obeyed Langmuir adsorption isotherm.
- Surface studies such as SEM, EDX supported to the adsorption of inhibitor on metal surface.
- Results obtained by PDP method and EIS method were in good agreement with one another.
- SASE emerged as a potential green corrosion inhibitor with maximum efficiency of 88.48% at 45 °C for 0.1g L⁻¹ of inhibitor.

References

1. Ovi J E O. Corrosion Resistance of Mg Mn Zn Ferrite in Hostile Environments. Nigerian Corrosion Journal, 1998, 1(1): 65-72
2. Tao Z, Zhang S, W.Li, Hou B. The role of metal cations in improving the inhibitive performance of hexamine on the corrosion of steel in hydrochloric acid solution. Corrosion Science, 2009, 51: 2588–2595
3. Singh A K, Quraishi M A. Study of some bidentate Schiff bases of isatin as corrosion inhibitors for mild steel in hydrochloric acid solution. International Journal of Electrochemical Science, 2012, 7:3222–3241
4. Singh D D N, Singh T B, Gaur B. The role of metal cations in improving the inhibitive performance of hexamine on the corrosion of steel in hydrochloric acid solution. Corrosion Science, 1995, 37: 1005–1019
5. Wang L. Inhibition of mild steel corrosion in phosphoric acid solution by triazole derivatives. Corrosion Science, 2006, 48: 608
6. Noor E. The inhibition of mild steel corrosion in phosphoric acid solutions by some N-heterocyclic compounds in the salt form. Corrosion Science, 2005, 47:33
7. Sanyal B. Organic compounds as corrosion inhibitors in different environments – a review. Prog Org Coat, 1981, 9:165
8. Obot I B, Obi-Egbedi N O. Ginseng Root: A new Efficient and Effective Eco-Friendly corrosion Inhibitor for Aluminum Alloy of type AA 1060 in Sulfuric acid Solution. International Journal of Electrochemical Science, 2009,4: 1277-1288
9. Obot I B, Obi-Egbedi N O. Ipomoea Involcrata as an Ecofriendly Inhibitor for Aluminum in Alkaline Medium. Portugaliae Electrochimicaal Acta, 2009, 27(4):517-524
10. Gupta V. Prospects and perspectives of natural plants products in medicine. Indian Journal of Pharmacology, 1994, 26:1-12

11. Deepa P, Padmalatha R. Corianbrun sativum L. – A noval green inhibitor for the corrosion inhibition of aluminium in 1M Phosphoric acid solution. *Journal of environmental Chemical engineering*,2013, 1:676–683
12. El Kadher A, El-Warraky J M, Abd el Aziz A M. Corrosion inhibition of mild steel by sodium tungstate in neutral solution part 1: behaviour in distilled water. *Br Corros Journal*. 1998,33:139–144
13. Li WH, He Q, Zhang S, Pei, CL, Hou B R. Some new triazole derivatives as inhibitors for mild steel corrosion in acidic medium. *Jour Appl Electrochem*, 2008,38: 289–295
14. Shahin M, Bilgic S, Yilmaz H. The inhibition effects of some cyclic nitrogen compounds on the corrosion of the steel in NaCl medium. *Appl Surf Sci*, 2003,195:1–7
15. Li WH, He Q, Zhang S, Pei, CL, Hou B R. Some new triazole derivatives as inhibitors for mild steel corrosion in acidic medium. *Journal Appl Electrochem*, 2008,38:289–295
16. Mansfeld F, Lin S, Kim K, Shih H. Pitting and Surface Modification of SiC/Al. *Journal of Corr Sci*, 1987,27: 997
17. Poornima T, Jagannatha N, Nithyananda A S. 3,4-dimethoxybenzaldehyde thiosemicarbazone as corrosion inhibitor for aged 18 Ni 250 grade maraging steel in 0.5M Sulfuric acid. *Journal Appl Electrochem*,2011, 41: 223
18. Poornima T, Jagannatha N, Nithyananda A S. Studies on corrosion of annealed and aged 18 Ni 250 grade maraging steel in sulphuric acid medium. *Portugal Electrochim Acta*, 2010,28:173–188
19. Ameer M A, Khamis E, Al-Senani G. Effect of temperature on stability of adsorbed inhibitors on steel in phosphoric acid solution. *Journal Appl Electrochem*, 2002, 32:149–156
20. Osman M M, El-Ghazawy RA, Al-Sabagh A M. Corrosion inhibitor of some surfactants derived from maleic–oleic acid adducts on mild steel in 1M H₂SO₄. *Mater Chem Phys*, 2003,80: 55–62
21. Oguzie E E, Njoku V O, Enenebeaku CK, Akalezi C O, Obi C. Effect of hexamethylpararosaniline chloride (crystal violet) on mild steel corrosion in acidic media. *Journal of Corros Sci*, 2008,50:3481
22. Ashassi-Sorkhabi H, Shaabani B, Seifzadeh D. Effect of some pyrimidinic Schiff bases on the corrosion of mild steel in hydrochloric acid solution. *Appl Surf Sci*, 2005,239,154–164
23. Bouklah M, Hammouti B, Lagrenee M, Bentiss F. Thermodynamic properties of 2,5-bis(4-methoxyphenyl)-1,3,4-oxadiazole as corrosion inhibitor for mild steel in normal sulfuric acid medium. *Corros Sci*, 2006,48:2831–2842
24. Sahin M, Bilgic S, Yilmaz H. The inhibition effects of some cyclic nitrogen compounds on the corrosion of the steel in NaCl mediums. *Appl Surf Sci*, 2002, 195:1-7
25. Soltani N, Behpour M, Ghoreishi S M, Naeimi H. Corrosion inhibition of mild steel in hydrochloric acid solution by double Schiff bases. *Corro Sci*, 2010,52:135-1361
26. Bentiss F, Traisnel M, Lagrenee M. Influence of 2,5-bis (4-imethylaminophenyl)-1,3,4-thiadiazole on corrosion inhibition of mild steel in acidic media. *Journal Appl Electrochem*, 2001, 31:41-48
27. Quraishi MA, Rawat J, Ajmal M. Dithiobiurets: a novel class of acid corrosion inhibitors for mild steel. *Appl Electrochem*, 2000,30: 745–751
28. Khaled KF, Hackerman N. Investigation of the inhibitive effect of ortho-substituted anilines on corrosion of iron in 1 M HCl solution. *Electrochem Acta*, 2003, 48:2715–2723
29. Singh AK, Quraishi M A. Effect of Cefazolin on the corrosion of mild steel in HCl solution. *Corrosion Science*, 2010, 52(1): 152–160
